

Supporting Information

Surface Modification of Indium-Tin Oxide with Functionalized Perylene Diimides: Characterization of Orientation, Electron-Transfer Kinetics and Electronic Structure

Yilong Zheng,¹ Anthony J. Giordano,² R. Clayton Shallcross,¹ Sean R. Fleming,¹ Stephen Barlow,² Neal R.

Armstrong,¹ Seth R. Marder,^{2*} S. Scott Saavedra^{1*}

¹Department of Chemistry & Biochemistry, University of Arizona, Tucson, AZ 85721

²School of Chemistry & Biochemistry and the Center for Organic Photonics and Electronics, Georgia
Institute of Technology, Atlanta, GA 30332-0400

* Authors to whom correspondence should be addressed:

saavedra@email.arizona.edu, seth.marder@chemistry.gatech.edu

1. Synthesis of PDI-phenyl-PA and PDI-diphenyl-PA	S-2
2. Aggregation of dissolved PDI-phenyl-PA and PDI-diphenyl-PA	S-7
3. Adsorption isotherms for PDI-PA films on ITO	S-8
4. Electrochemistry of dissolved and adsorbed PDI-PAs	S-9
5. Additional figures and tables	S-11
6. References	S-15

1. Synthesis of PDI-phenyl-PA and PDI-diphenyl-PA

1.1. General. The two phosphonic acids were synthesized as shown in Figure S1. Unless otherwise specified, reactions were conducted at room temperature utilizing reagent grade chemicals that were used as received without further purification. Compound I was synthesized according to the literature.¹ ^1H and $^{13}\text{C}\{^1\text{H}\}$ NMR spectra were acquired on either a Varian 300 MHz or 400 MHz spectrometer using the internal solvent peak as reference. $^{31}\text{P}\{^1\text{H}\}$ NMR spectra were measured using a Varian 400 MHz spectrometer using a capillary tube filled with a solution of 85% phosphoric acid ($\delta = 0$ ppm) as an external reference. Elemental analyses were conducted by Atlantic Microlabs, Atlanta, GA. Mass spectra were measured by the Georgia Institute of Technology Bioanalytic Mass Spectrometry Facility using either electron impact (EI) on a MicroMass AutoSpec M, or matrix-assisted laser desorption ionization (MALDI) on an Applied Biosystems 4700 Proteomics Analyzer.

1.2. Diethyl (4-aminophenyl)phosphonate (II). $\text{HP}(\text{O})(\text{OEt})_2$ (11.2 mL, 87.2 mmol), NEt_3 (6.1 mL, 43.6 mmol), and EtOH (100 mL) were added via syringe to a round-bottomed flask containing *p*-bromoaniline (10 g, 58.1 mmol), $\text{Pd}(\text{OAc})_2$ (0.6 g, 2.9 mmol), and PPh_3 (2.3 g, 8.7 mmol) under nitrogen. The reaction mixture was heated reflux for 72 h; upon cooling volatiles were removed under reduced pressure and the resulting off-white solid was purified by dissolving in a mixture of hexane/ethyl acetate (1:1), and precipitating by the addition of hexane. The solid was then further purified by column chromatography (silica gel eluting, CHCl_3 followed by 5% MeOH in CHCl_3 to produce II (3.0 g, 23%). The ^1H NMR spectrum was consistent with that reported in the literature.²

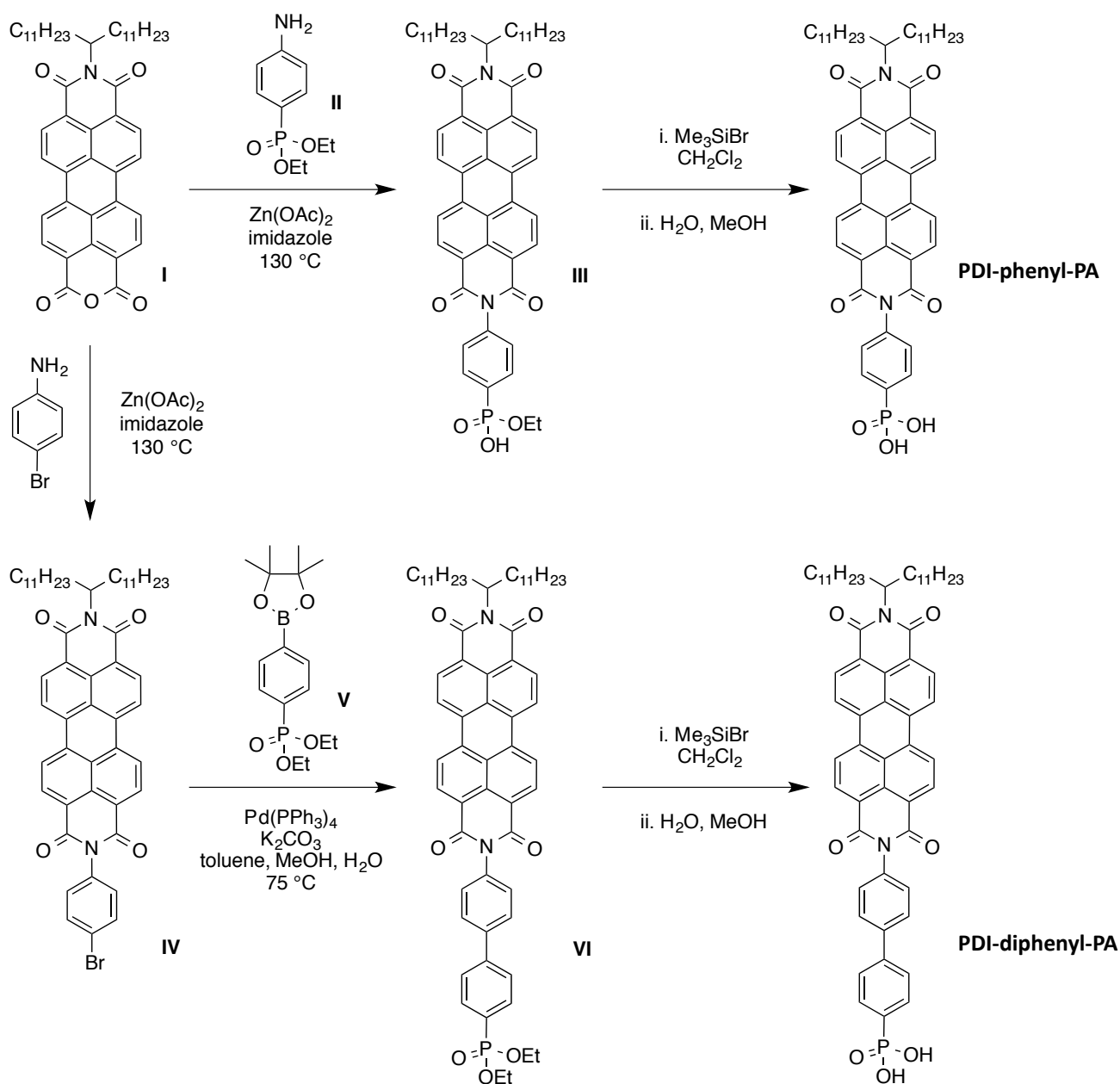


Figure S1. Synthesis of PDI-phenyl-PA and PDI-diphenyl-PA.

1.3. N-(4-(Ethoxy(hydroxy)phosphoryl)phenyl)-N'-(tricosan-12-yl)-perylene-3,4:9,10-bis(diethyl phosphonate), III. Compound **I** (0.50 g, 0.70 mmol), $\text{Zn}(\text{OAc})_2$ (0.10 g, 0.5 mmol), **II** (0.48 g, 2.1 mmol), and imidazole (4.29 g, 63.0 mmol) were combined in a pressure vessel, which was purged with nitrogen, sealed, and heated to $130\text{ }^\circ\text{C}$ for 3 h. Upon cooling, the mixture was diluted in CHCl_3 , and washed twice with 2 N aqueous HCl. The product was then purified by column chromatography

(silica gel, eluting with 10:1 CHCl₃/EtOH). Volatiles were removed under reduced pressure to afford a red solid, which was further purified by dissolving in minimal CHCl₃ and precipitating slowly with MeOH. The resulting solid was washed with MeOH, dried and afforded **III**, rather than the expected diethyl ester (0.50 g, 80%). ¹H NMR (400 MHz, THF-*d*₈) δ 8.44–8.27 (m, br, 8H), 7.90–7.85 (m, 2H), 7.47 (apparent d, 2H, *J* = 8.0 Hz), 5.14 (quint., 1H, *J* = 8.0 Hz), 4.12 (m, 2H), 2.00–1.88 (m, 2H), 1.45–1.18 (m, 42H), 0.87–0.83 (m, 6H). ¹³C{¹H} NMR (100 MHz, THF-*d*₈) δ 163.4, 139.8, 134.8, 134.1, 133.0, 132.9, 131.3, 130.4, 130.2, 126.3, 126.2, 124.0, 123.9, 62.59, 56.52, 33.5, 33.1, 30.9, 30.9, 30.8, 30.5, 28.5, 23.7, 17.1, 17.0, 14.6. ³¹P{¹H} NMR (162 MHz, THF-*d*₈) δ 20.01. MS(MALDI): *m/z* 897.4 (MH⁺). Elemental analysis calculated (found) for C₅₅H₆₅N₂O₇P: C 73.64 (73.54), H 7.30 (7.25), N 3.12 (3.15).

1.4. *N*-(4-Phosphonophenyl)-*N'*-(tricosan-12-yl)-perylene-3,4:9,10-bis(dicarboximide), PDI-phenyl-PA. Compound **III** (0.15 g, 1.7 mmol) was dissolved in dry CH₂Cl₂ (ca. 20 mL) and bromotrimethylsilane (1.0 mL, 7.5 mmol) was added via syringe. The reaction vessel was stoppered and stirred at room temperature overnight. Volatiles were then removed under reduced pressure and 10:1 MeOH/H₂O (ca. 20 mL) and CHCl₃ (ca. 20 mL) were added to the resulting thick oil; this mixture was then stirred overnight. Volatiles were then removed under reduced pressure and the resulting solid was purified by dissolving the solid in a minimal amount of CHCl₃ and precipitating with MeOH to afford a dark red solid (0.12 g, 83%). ¹H NMR (400 MHz, THF-*d*₈) δ 8.18–8.07 (m, 8H), 7.95–7.90 (m, 2H), 7.55 (m, 2H), 5.06 (quint., 1H, *J* = 7.2 Hz), 2.01–1.92 (m, 2H), 1.42–1.27 (m, 36H), 0.88–0.84 (m, 6H). ³¹P{¹H} NMR (162 MHz, THF-*d*₈) δ 16.01. HRMS (MALDI) calculated (found) for C₅₃H₆₂N₂O₇P (MH⁺): 869.4295 (869.4252). Elemental analysis calculated (found) for C₅₃H₆₁N₂O₇P.H₂O: C 71.76 (71.55), H 7.16 (6.98), N 3.16 (3.19).

1.5. N-(4-Bromophenyl)-N'-(tricosan-12-yl)-perylene-3,4:9,10-bis(dicarboximide), IV.

Compound I (0.60 g, 0.84 mmol), Zn(OAc)₂ (0.12 g, 0.55 mmol), 4-bromoaniline (0.48 g, 2.1 mmol), and imidazole (5.14 g, 68.0 mmol) were combined in a pressure vessel, which was purged with nitrogen, sealed, and heated to 130 °C overnight. Upon cooling, the mixture was diluted in CHCl₃, and washed twice with 2 N aqueous HCl. Volatiles were removed under reduced pressure and the residue was purified by column chromatography on silica gel, eluting with CHCl₃/CH₂Cl₂ (1:1), to give a red solid (0.40 g, 78%). ¹H NMR (400 MHz, CDCl₃) δ 8.75-7.63 (m, 8H); 7.71 (d, *J* = 7.6 Hz, 2H); 7.25 (d, *J* = 8.4 Hz, 2H); 5.19 (quint., *J* = 5.2 Hz, 1H); 2.30-2.20 (m, 2H); 1.93-1.80 (m, 2H); 1.40-1.10 (m, 36H); 0.84 (t, *J* = 6.8 Hz, 6H). HRMS (MALDI) calculated (found) for C₅₃H₆₀BrN₂O₄ (MH⁺): 867.3736 (867.3732). Elemental analysis calculated (found) for C₅₃H₅₉BrN₂O₄: C 73.34 (73.64), H 6.85 (6.77), N 3.12 (3.31).

1.6. Diethyl (4-(4,4,5,5-tetramethyl-1,3,2-dioxaborolan-2-yl)phenyl)phosphonate, V.

Bis(pinacolato)diboron (2.63 g, 10.4 mmol), 1,1'-bis(diphenylphosphino)ferrocene palladium dichloride dichloromethane complex (0.23 g, 0.3 mmol), and potassium acetate (1.77 mL, 28.4 mmol) were dissolved in anhydrous dimethyl sulfoxide (45 mL) under nitrogen; diethyl (4-bromophenyl)phosphonate (2.77 g, 9.45 mmol) was added and the mixture was heated to 80 °C for 30 h. The product was extracted with EtOAc, washed with water, dried over MgSO₄, and filtered. Volatiles were removed under reduced pressure and the residue was purified using Kugelrohr distillation (60 mTorr, 175 °C) to afford **V** as an off-white solid (1.15 g, 36%). ¹H NMR (400 MHz, CDCl₃) δ 7.91–7.88 (m, 2H), 7.83–7.78 (m, 2H), 4.19–4.01 (m, 4H), 1.35 (s, 12H), 1.31 (t, 6H, *J* = 7.2 Hz). ¹³C{¹H} (100.58 MHz, CDCl₃) δ 134.8 (d, *J* = 14.5 Hz), 132.1, 131.1 (d, *J* = 9.6 Hz), 130.2, 84., 62.3 (d, *J* = 5.3 Hz), 25.1, 16.5 (d, *J* = 6.4 Hz). ³¹P{¹H} NMR (161.91 MHz, CDCl₃) δ 19.16. HRMS(EI)

calculated for $C_{16}H_{26}BO_5P$ (M^+) (found): 340.1611 (340.1615). Elemental analysis calculated (found) for $C_{16}H_{26}BO_5P$: C 56.49 (56.45), H 7.70 (7.73).

1.7. *N*-(4'-(Diethoxyphosphoryl)-[1,1'-biphenyl]-4-yl)-*N'*-(tricosan-12-yl)-perylene-3,4:9,10-bis(dicarboximide), VI. A mixture of **IV** (0.3 g, 0.4 mmol), **V** (0.5 g, 1.5 mmol), and $Pd(PPh_3)_4$ (0.08 g, 0.1 mmol) were dissolved in a mixture of toluene (50 mL), methanol (14 mL). K_2CO_3 (14 mL of a 2 M aqueous solution) was added and the reaction mixture was stirred under nitrogen at 75 °C for 15 h with exclusion of light. After cooling the reaction mixture was washed twice with deionized water and twice with brine, dried over $MgSO_4$, and filtered. The volatiles were removed under reduced pressure and the resulting red solid was dissolved in a minimal amount of $CHCl_3$ and precipitated slowly after addition of MeOH. The precipitate was washed with MeOH and filtered to afford the title compound as a red solid (0.29 g, 82%). 1H NMR (400 MHz, THF- d_8) δ 8.71–8.67 (m, 4H), 8.58–8.51 (m, br, 4H), 7.92–7.83 (m, 6H), 7.52 (d, 2H, $J = 8.0$ Hz), 5.24–5.16 (m, 1H), 4.16–4.04 (m, 4H), 2.37–2.31 (m, 2H), 1.92–1.84 (m, 2H), 1.41–1.16 (m, 42H), 0.86–0.83 (m, 6H). $^{13}C\{^1H\}$ NMR (100 MHz, THF- d_8) δ 163.6, 145.1, 145.1, 140.9, 136.9, 134.9, 134.5, 133.4, 133.3, 131.4, 130.9, 130.8, 129.8, 129.7, 128.9, 128.5, 128.1, 127.9, 126.5, 126.4, 124.2, 62.4 (d, $J = 6.0$ Hz), 55.4, 33.5, 33.1, 30.9, 30.9, 30.8, 30.8, 30.8, 30.5, 23.7, 17.0 (d, $J = 6.0$ Hz), 14.6. $^{31}P\{^1H\}$ NMR (162 MHz, $CDCl_3$) δ 18.58. HRMS(MALDI) calculated for $C_{63}H_{74}N_2O_7P$ (MH^+) (found): 1001.5234 (1001.5212).

1.8. *N*-(4'-Phosphono-[1,1'-biphenyl]-4-yl)-*N'*-(tricosan-12-yl)-perylene-3,4:9,10-bis(dicarboximide), PDI-biphenyl-PA. Bromotrimethylsilane (1.5 mL, 11.4 mmol) was added to a solution of **VI** (0.16 g, 0.2 mmol) in dry CH_2Cl_2 (ca. 10 mL) via syringe. The reaction vessel was stoppered and stirred at room temperature overnight. The volatiles were removed under reduced pressure; 10:1 MeOH/ H_2O (ca. 20 mL) and $CHCl_3$ (20 mL) were added to the residue and the mixture was stirred

overnight. Volatiles were removed under reduced pressure and the resulting solid was recrystallized by dissolving the solid in a minimal amount of CHCl_3 and precipitating with MeOH to afford a dark red solid (0.12 g, 86%). NMR spectra were severely broadened at both room and elevated temperature in a variety of solvents, presumably due to aggregation. HRMS(MALDI) calculated for $\text{C}_{59}\text{H}_{66}\text{N}_2\text{O}_7\text{P}$ (M^+) (found): 945.4608 (945.4592). Elemental analysis calculated (found) for $\text{C}_{59}\text{H}_{65}\text{N}_2\text{O}_7\text{P}\cdot\text{H}_2\text{O}$: C 73.58 (73.02), H 7.01 (6.89), 2.91 (2.95).

2. Aggregation of dissolved PDI-phenyl-PA and PDI-diphenyl-PA

PDIs are prone to aggregate in solution, and adsorption of aggregated forms could affect the structure of an adsorbed monolayer on ITO. Aggregation of PDIs is characterized by broadened absorbance bands and a decreased ratio of the 0-0/0-1 absorbance bands.³⁻⁸ A PDI solution that produces a 0-0/0-1 ratio of ca. 1.6 is considered monomeric.⁶ Here, different solvents, solvent mixtures and solvent additives were tested to minimize the aggregation of dissolved PDI-phenyl-PA and PDI-diphenyl-PA. Tetrabutylammonium hydroxide (TBA-OH) was used as solution additive to reduce PDI-phenyl-PA and PDI-diphenyl-PA aggregation, which may be due in part to PA-PA interactions. Absorbance spectra of PDI-phenyl-PA dissolved in different solvents are shown in Figure S2. The highest 0-0/0-1 absorbance band ratio, 1.62, was observed using 90% DMF + 10% CHCl_3 containing TBA-OH in an equimolar ratio with PDI-phenyl-PA. Similar results were obtained with dissolved PDI-diphenyl-PA; the highest 0-0/0-1 ratio was 1.61 using 50% DMF + 50% CHCl_3 containing TBA-OH in an equimolar ratio with PDI-diphenyl-PA. Those solution conditions were used to deposit solution adsorbed (SA) PDI films on ITO electrodes.

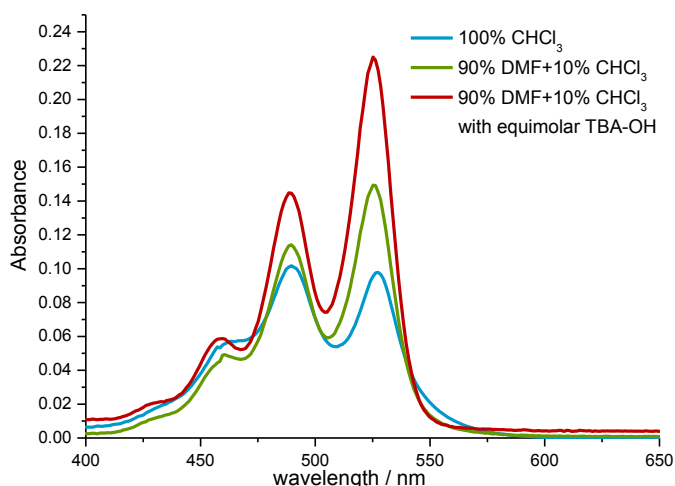


Figure S2. Absorption spectra of 20 μM PDI-phenyl-PA dissolved in CHCl_3 (blue line), 90% DMF + 10% CHCl_3 (green line) and 90% DMF + 10% CHCl_3 containing 20 μM tetrabutylammonium hydroxide (TBA-OH). Spectra were acquired in a 1 cm path length cuvette using a Shimadzu UV-2401PC spectrophotometer.

3. Adsorption isotherms for PDI-PA films on ITO

The adsorption of PDI-PAs onto ITO electrodes was monitored using ATR spectroscopy. Figure S3A shows spectra acquired as a function of time after injecting a 20 μM solution of PDI-phenyl-PA in 90% DMF+10% CHCl_3 with equimolar TBA-OH in the flow cell. The absorbance of the most intense band (λ_{max} at 460 nm) of PDI-phenyl-PA, plotted in Figure S3B, increased and reached a plateau around 40-60 min after injection, indicating the ITO surface was saturated. After flushing the cell with solvent to remove the incubation solution and any weakly physisorbed molecules, the absorbance declined very little (red triangle in Fig. S3B), showing that the molecules were strongly adsorbed. For PDI-diphenyl-PA, the behavior was similar except that it took about 70-90 min for saturation to occur, and the absorbance value at saturation was slightly less than that observed for PDI-phenyl-PA. Based on these results, adsorption times of 1 h and 2 h were used to prepare SA PDI-phenyl-PA and PDI-diphenyl-PA films, respectively, for all subsequent electrochemical, spectroscopic, and spectroelectrochemical characterization.

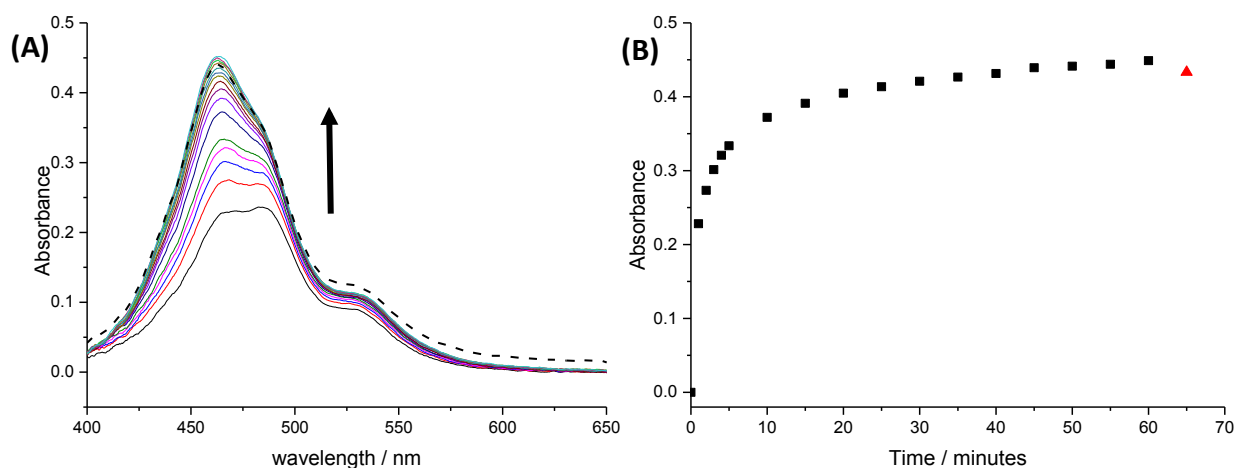


Figure S3. (A) TM polarized ATR spectra (solid lines) acquired as a function of time after a 20 μM solution of PDI-phenyl-PA was injected into an ATR flow cell containing an ITO waveguide. The arrow indicates the evolution of the spectra with increasing incubation time. The dashed line is the spectrum acquired after flushing the cell with pure CHCl_3 . (B) Absorbance at 460 nm monitored as a function of time during the adsorption process (black squares). The absorbance value measured after flushing the flow cell with solvent is also shown (red triangle).

4. Electrochemistry of dissolved and adsorbed PDI-PAs.

The effects of solvents and surface adsorption on the reduction potential of both PDI-PAs was investigated. Figure S4A shows diffusion-controlled cyclic voltammograms (CVs) of PDI-PAs dissolved in solution with/without TBA-OH, while Figure S4B shows the CVs of SA PDI-phenyl-PA and SA PDI-diphenyl-PA films on ITO. All voltammograms exhibited two reversible reduction steps corresponding to the formation of PDI anion radical ($\text{PDI}^{\cdot-}$) and PDI dianion (PDI^{2-}). Table S1 summarizes the first and second reduction midpoint potentials ($E^{0'}$) of dissolved and adsorbed PDI-PAs. Considering that the standard deviation of measuring a midpoint potential is about 0.05 V, all five measurements were equivalent. This result shows that the reduction midpoint potentials of the PDI-PAs were unaffected by linker length, addition of TBA-OH, or adsorption on ITO.

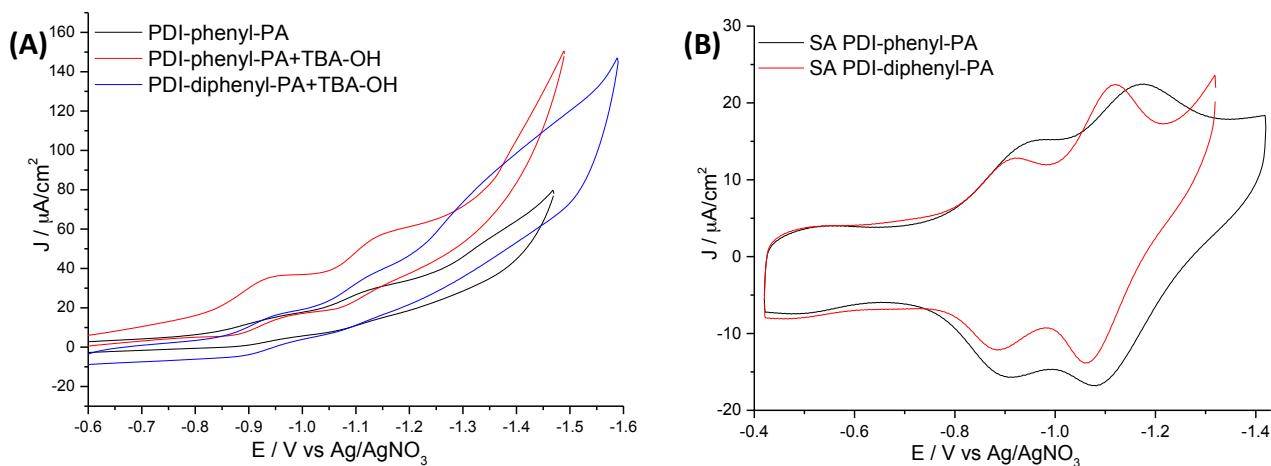


Figure S4. (A) Diffusion controlled CVs of PDI-phenyl-PA (black line), PDI-phenyl-PA with equimolar ratio of TBA-OH (red line) and PDI-diphenyl-PA with equimolar ratio of TBA-OH (blue line). The PDI-PA concentration was 100 μM and the working electrode was platinum. The electrolyte was 0.1 M TBAP in chloroform and the scan rate was 0.5 V/s. (B) CVs of SA PDI films on ITO. The electrolyte was 0.1 M TBAP in chloroform and the scan rate was 0.5 V/s.

Table S1. Redox potentials of dissolved PDI-PAs and SA PDI-PA films.^{a,b}

	PDI-phenyl-PA	PDI-phenyl-PA ^c	PDI-diphenyl-PA ^c	SA phenyl-PDI	SA diphenyl-PDI
$E^{0'}$, 1 st reduction	-0.92	-0.93	-0.93	-0.92	-0.90
$E^{0'}$, 2 nd reduction	-1.09	-1.11	-1.09	-1.11	-1.08

^a Potentials are stated vs. the Ag/AgNO_3 pseudo-reference electrode, which was calibrated using the ferrocene/ferricenium (Fc/Fc^+) redox couple. The $E^{0'}$ of Fc/Fc^+ was 0.11 V vs. Ag/AgNO_3 .

^b Analysis conditions are given in Figure S4.

^c Containing equimolar TBA-OH.

5. Additional figures and tables

Table S2. R_s and C_{dl} for PDI-PA films measured by impedance spectroscopy.^a

	SA PDI-diphenyl-PA	SA PDI-phenyl-PA	SC PDI-phenyl-PA
R_s ($\Omega \cdot \text{cm}^2$)	13 ± 3	14 ± 2	14 ± 2
C_{dl} ($\mu\text{F}/\text{cm}^2$)	16 ± 2	15 ± 1	14 ± 2

^a $n = 3$ for all measurements.

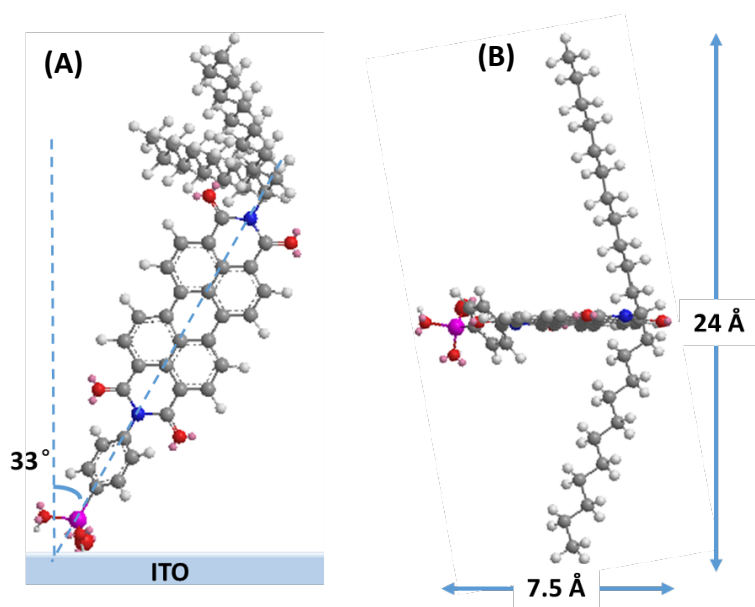


Figure S5. Side view (A) and top view (B) of a 3D representation of a PDI-phenyl-PA molecule placed on an ITO substrate at a tilt angle of 33° relative to the surface normal to the ITO surface plane. The structure was generated using MM2 energy minimization in ChemBio 3D software (Perkin-Elmer).

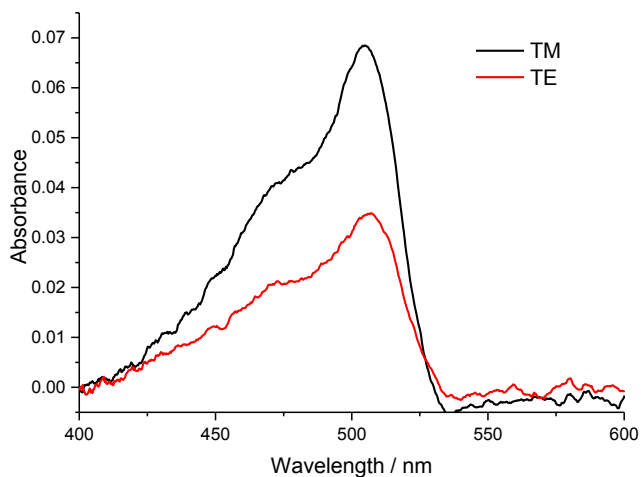


Figure S6. ATR spectra of a dextran-fluorescein film adsorbed on an ITO electrode in TM (black) and TE (red) polarizations. Assuming that the orientation distribution of the fluorescein absorption dipoles is random, the difference in absorbance is due to the unequal interfacial electric field intensities in TE and TM polarizations.

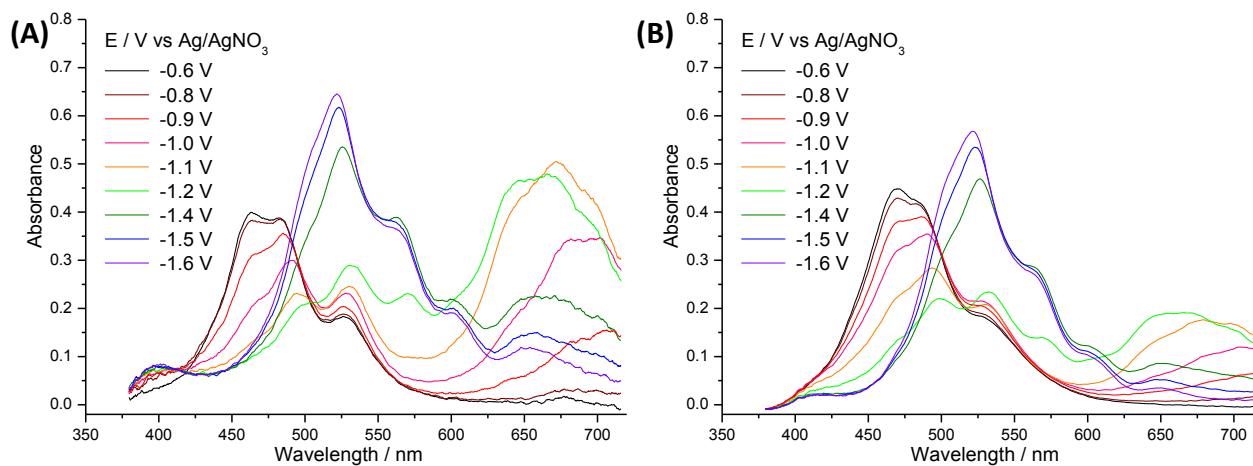


Figure S7. Potential-dependent ATR spectra of a (A) SA PDI-diphenyl-PA film and (B) a SC PDI-phenyl-PA film on ITO acquired in TM polarization from -0.6 V to -1.6 V versus a Ag/AgNO₃ pseudo-reference electrode.

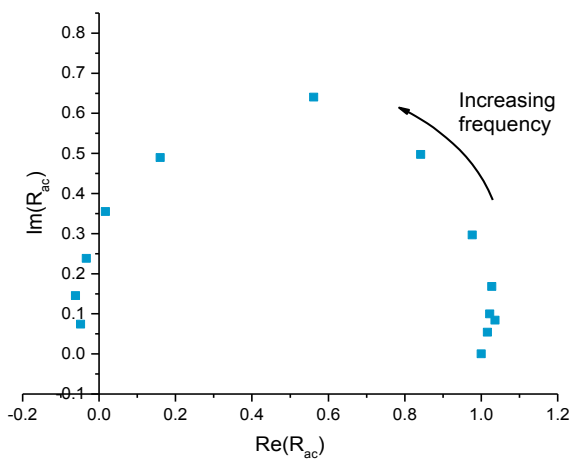


Figure S8. A complex plane plot for normalized imaginary ($\text{Im}(R_{ac})$) versus real components ($\text{Re}(R_{ac})$) of electroreflectance for a SA PDI-phenyl-PA film measured at 460 nm in TM polarization. The frequency where $\text{Re}(R_{ac})$ goes to zero is used to estimate $k_{s,opt}$.

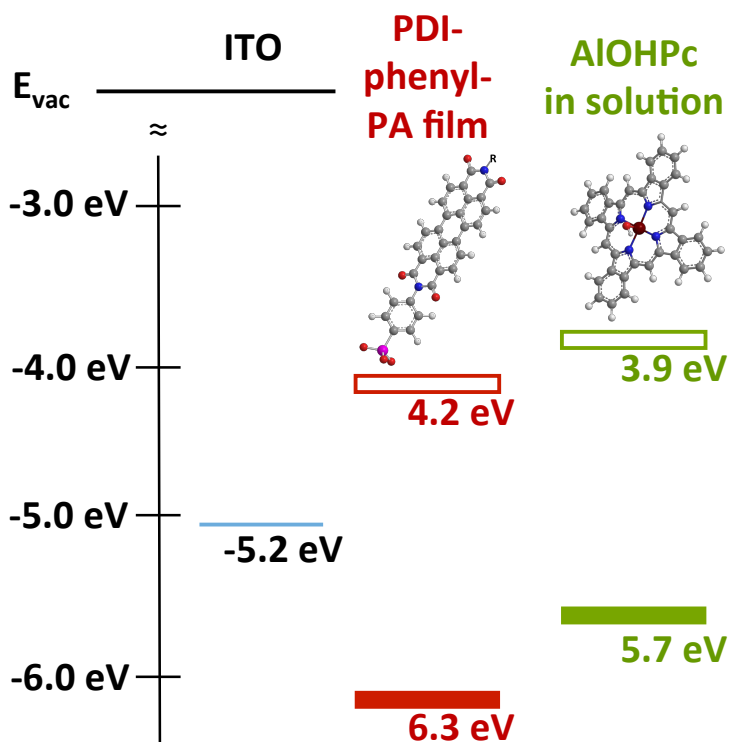


Figure S9. Energy level alignment of the components in the photoelectrochemical cell. The open rectangles and associated values represent E_{LUMO} . The filled rectangles and associated values represent E_{HOMO} . The Fermi energy of ITO, indicated by the solid blue line, was controlled by the applied potential.

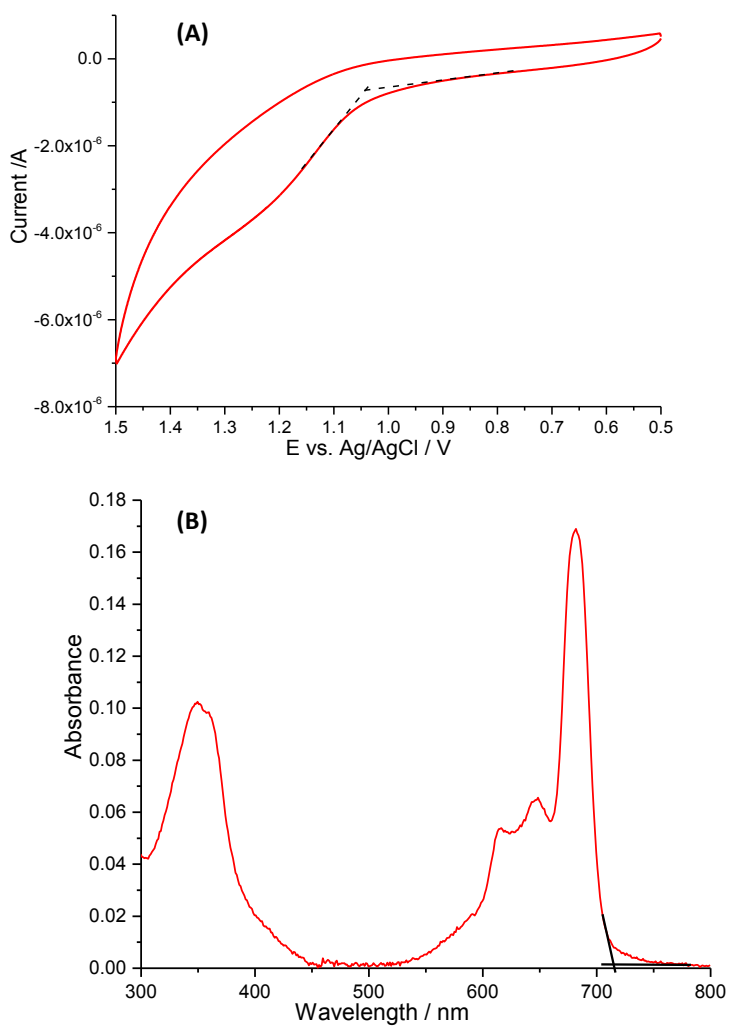


Figure S10. (A) Diffusion controlled cyclic voltammogram of AIOHPc dissolved in 1:1 (v/v) acetonitrile:pyridine (100 μM). The supporting electrolyte was 0.1M TBAP and the scan rate was 100 mV/s. The onset of the oxidation was estimated by extrapolation (dashed black lines) of the current to the baseline and used to estimate the HOMO of AIOHPc. (B) UV-visible absorbance spectrum of AIOHPc dissolved in 1:1 (v/v) acetonitrile:pyridine (ca. 10 μM). The low energy onset was estimated by extrapolation (solid black lines) of the absorbance to the baseline and used to estimate the band gap of AIOHPc.

6. References

- (1) Ahrens, M. J.; Kelley, R. F.; Dance, Z. E. X.; Wasielewski, M. R. Photoinduced Charge Separation in Self-Assembled Cofacial Pentamers of Zinc-5,10,15,20-tetrakis(perylene-3,9,10,16-tetracarboxylic diimide)porphyrin. *Phys. Chem. Chem. Phys.* **2007**, *9*, 1469-1478.
- (2) Kohler, M. C.; Sokol, J. G.; Stockland Jr, R. A. Development of a Room Temperature Hiraio Reaction. *Tetrahedron Lett.* **2009**, *50*, 457-459.
- (3) Zhao, Q.; Zhang, S.; Liu, Y.; Mei, J.; Chen, S.; Lu, P.; Qin, A.; Ma, Y.; Sun, J. Z.; Tang, B. Z. Tetraphenylethynyl-Modified Perylene Bisimide: Aggregation-Induced Red Emission, Electrochemical Properties and Ordered Microstructures. *J. Mater. Chem.* **2012**, *22*, 7387.
- (4) Würthner, F.; Thalacker, C.; Diele, S.; Tschierske, C. Fluorescent J-Type Aggregates and Thermotropic Columnar Mesophases of Perylene Bisimide Dyes. *Chem. Eur. J.* **2001**, *7*, 2245-2253.
- (5) Würthner, F.; Kaiser, T. E.; Saha-Moeller, C. R. J-Aggregates: From Serendipitous Discovery to Supramolecular Engineering of Functional Dye Materials. *Angew. Chem. Int. Ed.* **2011**, *50*, 3376-3410.
- (6) Liu, Y.; Wang, K.-R.; Guo, D.-S.; Jiang, B.-P. Supramolecular Assembly of Perylene Bisimide with β -Cyclodextrin Grafts as a Solid-State Fluorescence Sensor for Vapor Detection. *Adv. Funct. Mater.* **2009**, *19*, 2230-2235.
- (7) Jiang, B. P.; Guo, D. S.; Liu, Y. Self-Assembly of Amphiphilic Perylene-Cyclodextrin Conjugate and Vapor Sensing for Organic Amines. *J. Org. Chem.* **2010**, *75*, 7258-7264.
- (8) Chen, Z.; Baumeister, U.; Tschierske, C.; Würthner, F. Effect of Core Twisting on Self-Assembly and Optical Properties of Perylene Bisimide Dyes in Solution and Columnar Liquid Crystalline Phases. *Chem. Eur. J.* **2007**, *13*, 450-465.